Support information

3D structural lithium alginate-based gel polymer electrolytes with superior high rate long cycling performance for High-energy lithium metal batteries

Xin Wen[a], Qinghui Zeng[a], Jiazhu Guan[a] , Wen Wen[a], Pingping Chen[a], Zhenfeng Li[a], Yu Liu[a], Anqi Chen[a], Xiangfeng Liu [a], Wei Liu [a]*, Shangtao Chen[b]*, Liaoyun Zhang[a]*

[a] *University of Chinese Academy of Sciences, Beijing 100049, China*
[b] *Synthetic, Resin Lab., Petrochemical Research institute, Beijing 102206, China*
E-mails: zhangly@ucas.ac.cn; chenst7890@petrochina.com.cn; liuwei@ucas.ac.cn

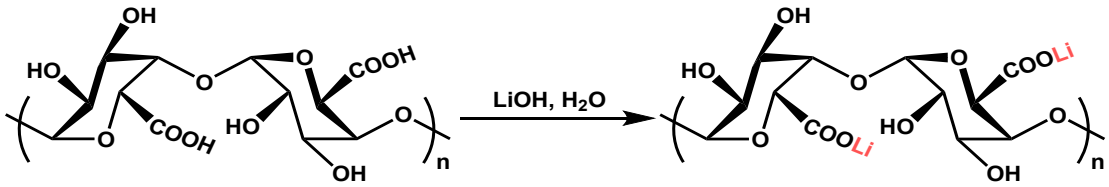

Fig. S1 Synthesis of lithium alginate.

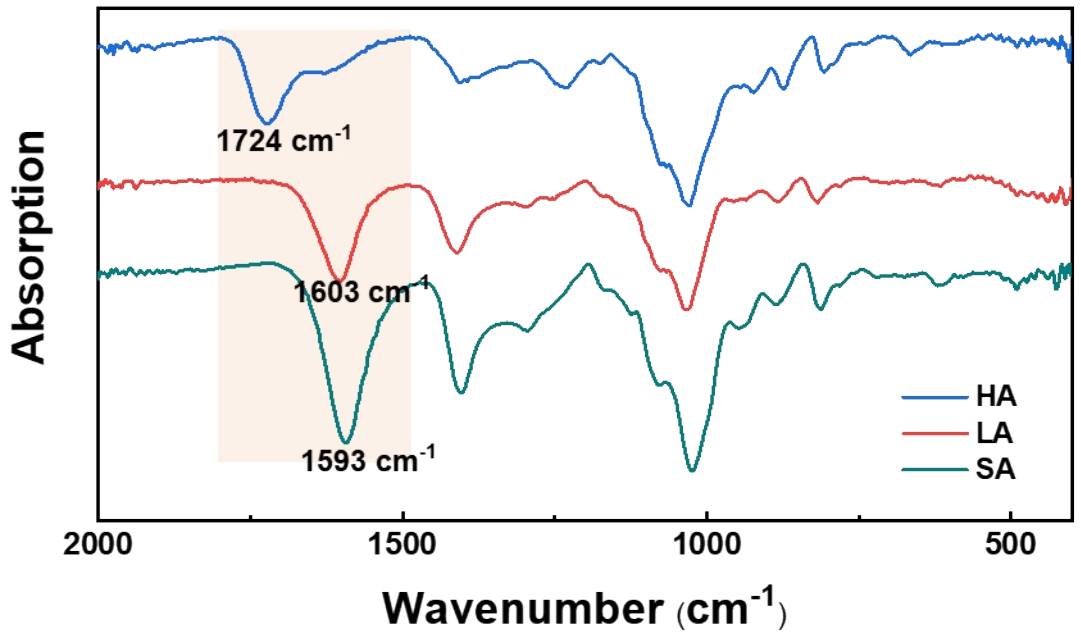

Fig. S2 IR spectra of alginate acid (HA), lithium alginate (LA), and sodium alginate (SA).

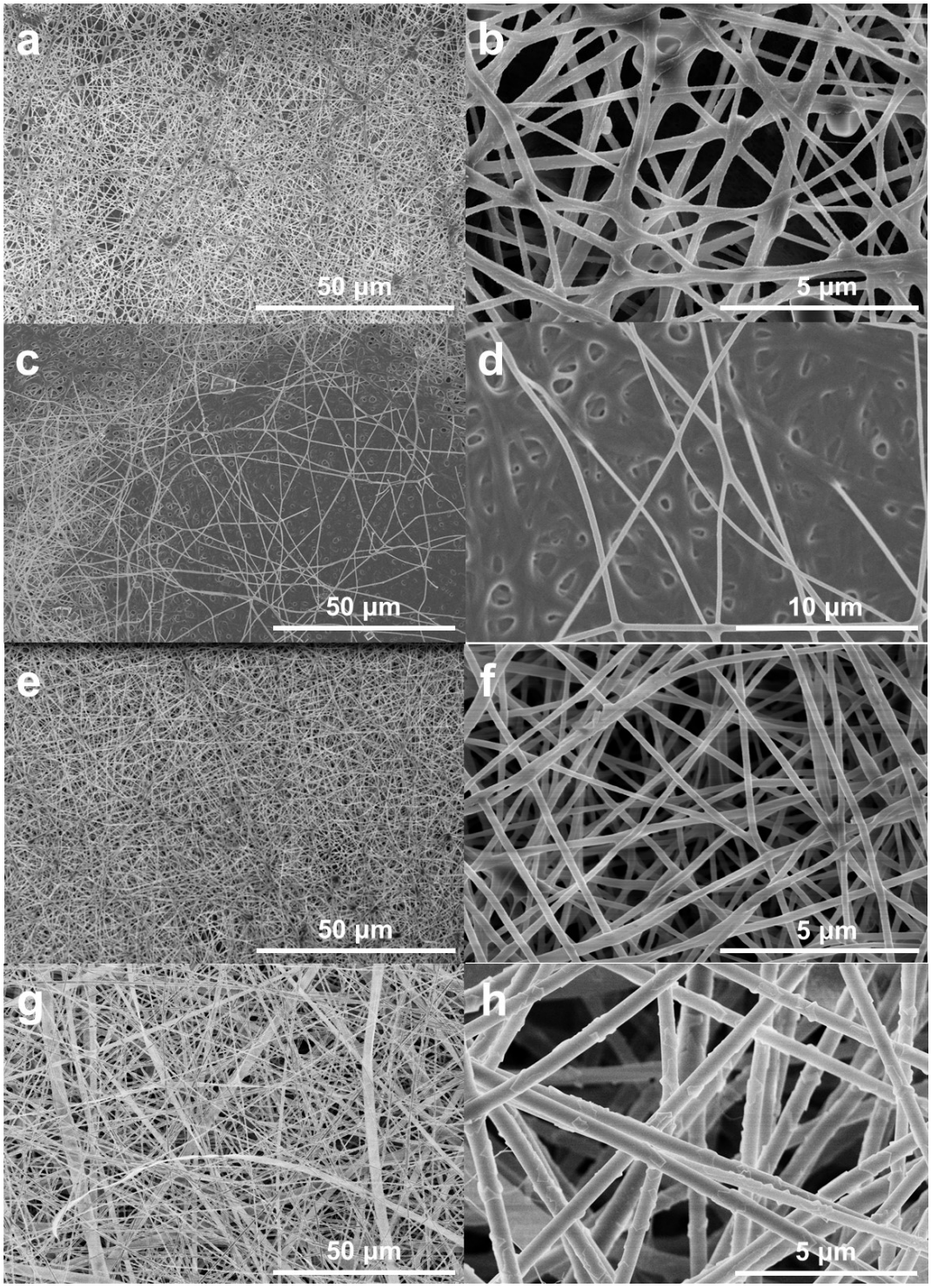

Fig. S3 SEM images of the surface of composite membranes (a), (b) LA-PEO-PAM-2-1-1, (c), (d) LA-PEO-PAM-4-1-1, (e), (f) LA-PEO-3-2, and (g), (h) LA-PAM-3-2.

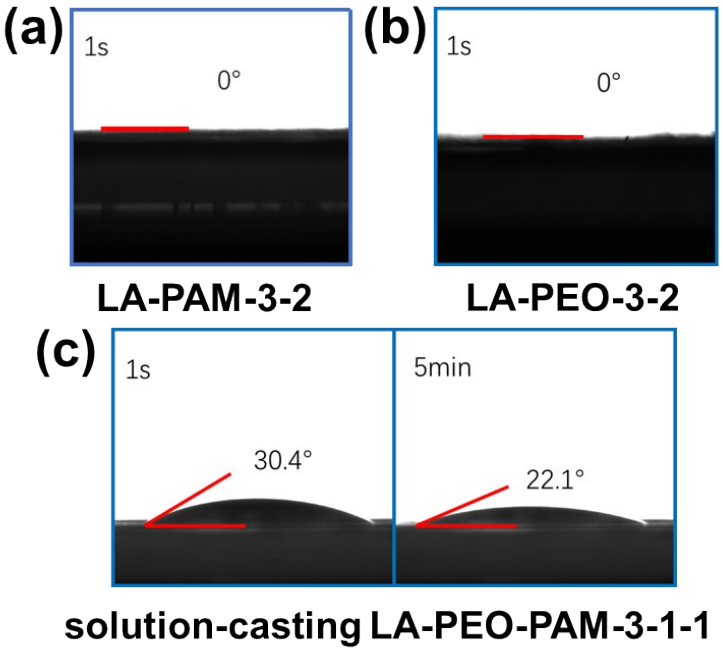

Fig. S4 Surface contact angles of 1M LiTFSI DMC/EC (1:1 vol%) with (a) electrospinning LA-PAM-3-2 membrane, (b) electrospinning LA-PEO-3-2 membrane, and (c) solution-casting LA-PEO-PAM-3-1-1 membrane, electrospinning, respectively.

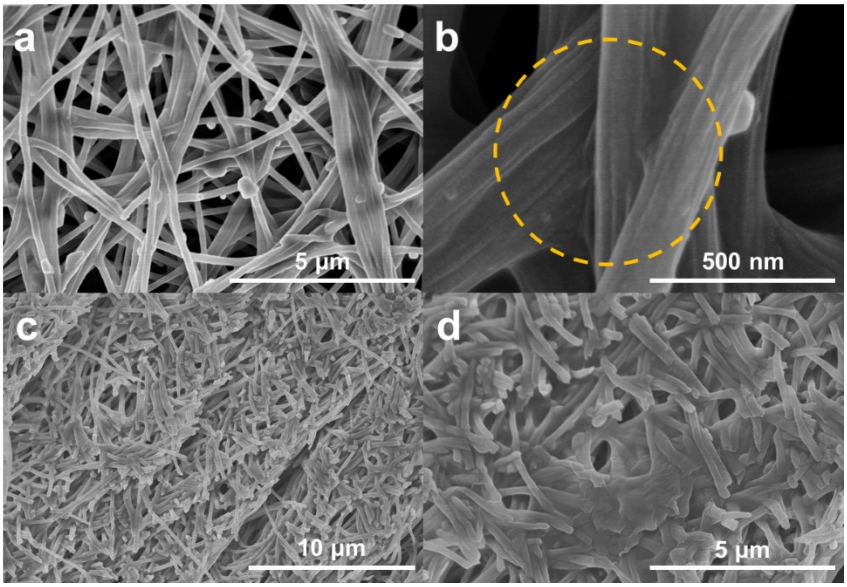

Fig. S5 SEM images of (a), (b) the surface and (c), (d) the cross-section of electrospinning composite membrane LA-PEO-PAM-3-1-1 after soaking liquid electrolyte.

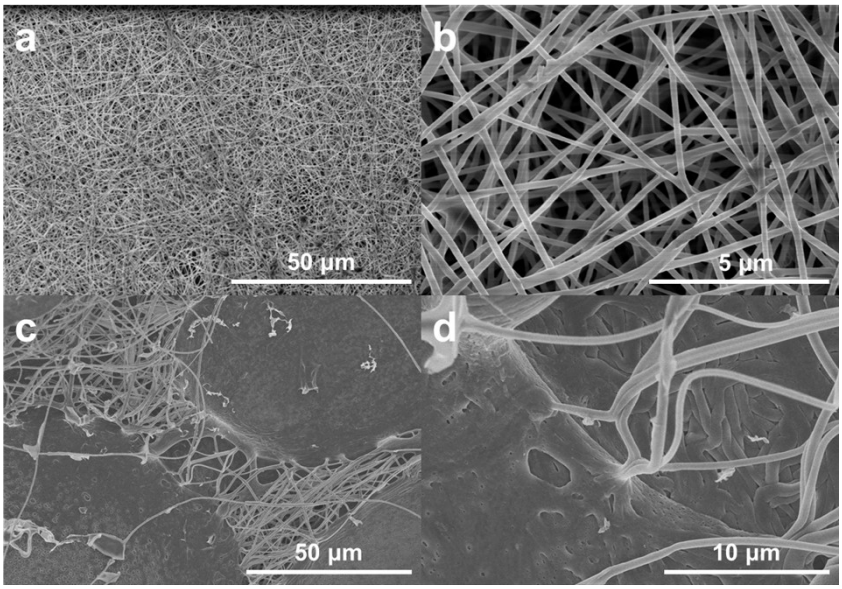

Fig. S6 SEM images of (a), (b) the surface and (c), (d) the cross-section of electrospinning composite membrane LA-PEO-3-2 after soaking liquid electrolyte.

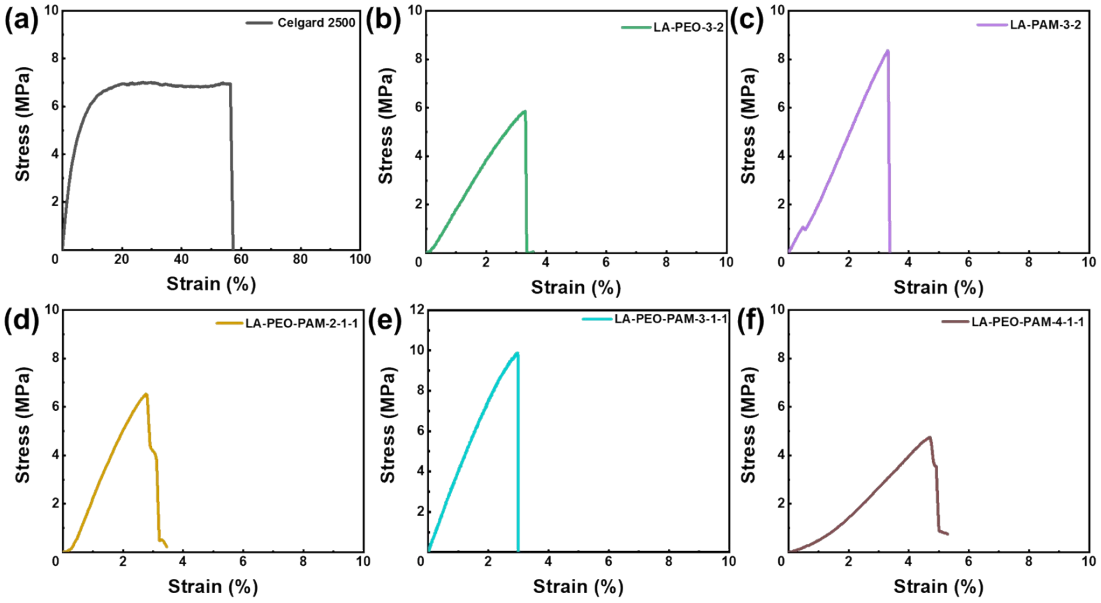

Fig. S7 Stress-Strain curves of (a) Celgard 2500, (b) electrospinning LA-PEO-3-2 membrane, (c) electrospinning LA-PAM-3-2 membrane, (d) electrospinning LA-PEO-PAM-2-1-1 membrane, (e) electrospinning LA-PEO-PAM-3-1-1 membrane, and (f) electrospinning LA-PEO-PAM-4-1-1 membrane.

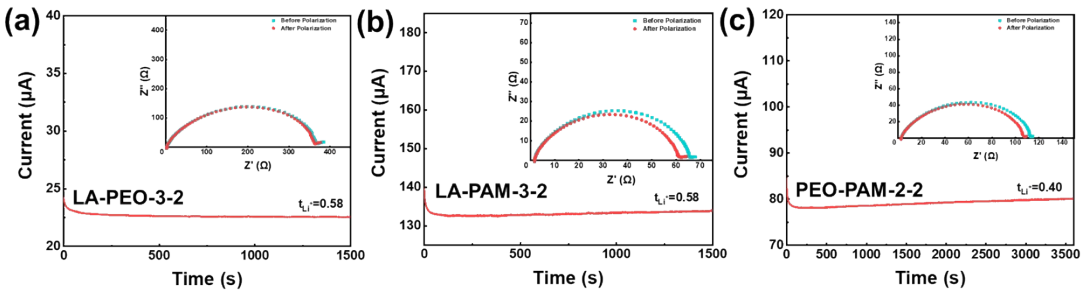

Fig. S8 Chronoamperometry curves and AC impedance spectra before and after polarization for composite electrolytes (a) LA-PEO-3-2, (b) LA-PAM-3-2, and (c) PEO-PAM-2-2.

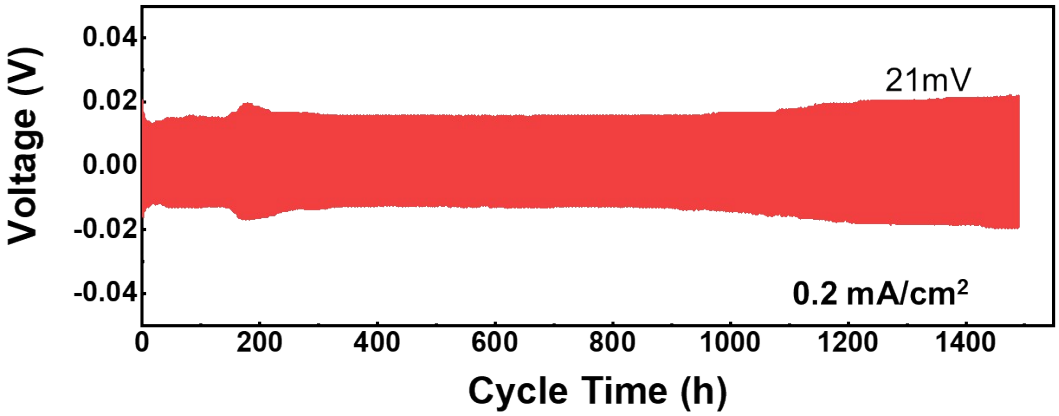

Fig. S9 Galvanostatic cycles for Li/ LA-PEO-PAM-3-1-1/Li cells at 0.2 mA cm^{-2} and 0.2 mAh cm^{-2}.

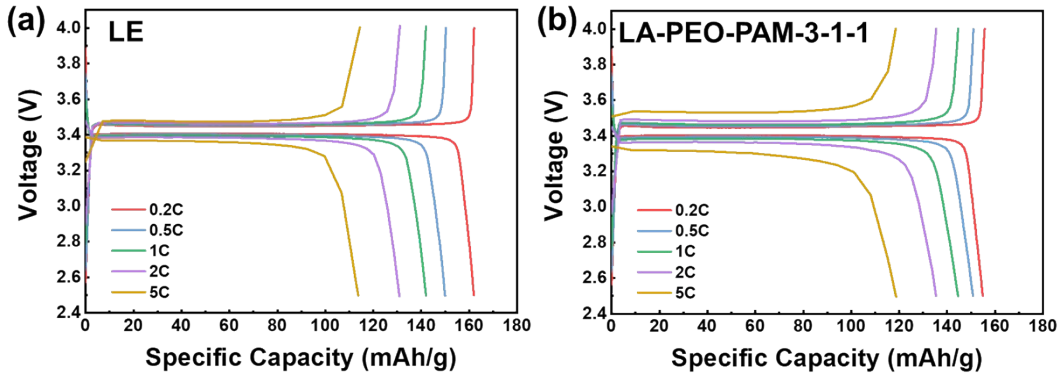

Fig. S10 (a) LFP/LE/Li and (b) LFP/LA-PEOPAM-3-1-1/Li cells at different rates.

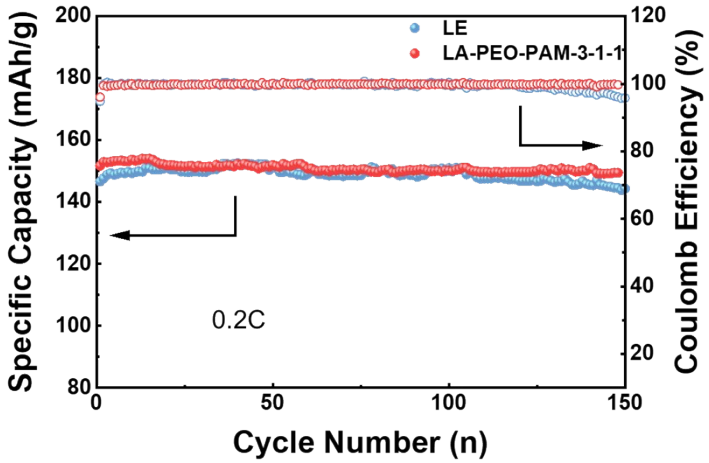

Fig. S11 Cycle performance test curves of LFP/LE/Li and LFP/LA-PEOPAM-3-1-1/Li cells at 0.2 C.

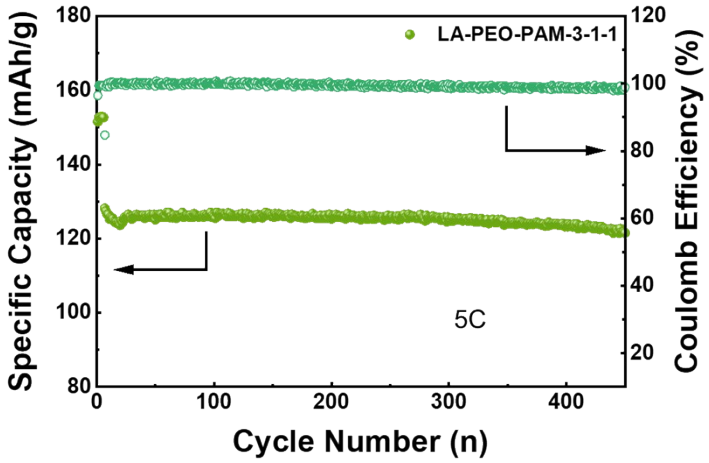

Fig. S12 Cycle performance test curve of LFP/LA-PEOPAM-3-1-1/Li cell at 5 C.

Fig. S13 Image of LFP/LA-PEO-PAM-3-1-1/Li button cell powering 3 LED bulbs in parallel.

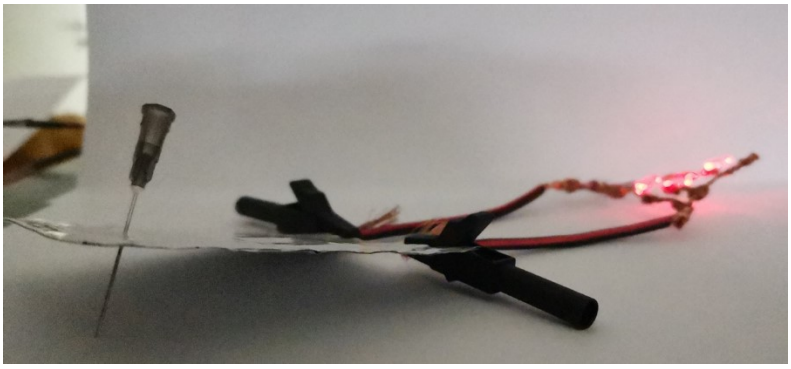

Fig. S14 Image of LFP/LA-PEO-PAM-3-1-1/Li pouch cell powering 3 LED bulbs in parallel at piercing.

Table. S1 The porosity of Celgard 2500 separator and LA-PEO-PAM-3-1-1 composite membrane.

Membrane	**Thickness**	**Mass before**	**Mass after**	**Porosity (ΔP, %)**

	(h, mm)	soaking (m_0, mg)	soaking (m_1, mg)		
Celgard 2500	0.025	4.1	6.1	35.9	35.9 (average)
	0.025	3.6	5.7	37.7	
	0.025	3.6	5.5	34.1	
LA-PEO-PAM-3-1-1 (electrospinning)	0.225	14.5	59.9	90.6	89.1 (average)
	0.213	12.5	54.0	87.5	
	0.181	7.2	43.2	89.3	

Table. S2 Absorptivity of each composite membrane to 1 M LiTFSI DMC/EC (1:1, v/v).

Composite membrane	**Mass before soaking (m_0, mg)**	**Mass after soaking (m_s, mg)**	**Absorptivity (ΔW, wt%)**
Celgard 2500	3.2	6.0	88
LA-PAM-3-2	6.7	35.9	436
LA-PEO-3-2	12.1	61.7	401
LA-PEO-PAM-3-1-1 (electrospinning)	9.0	52.4	482
LA-PEO-PAM-3-1-1 (solution-casting)	30.9	33.7	9

Table. S3 The test values of mechanical property from Stress-Strain curves.

Composite membrane	Tensile strength (MPa)	Young's Modulus (MPa)	Elongation at break (%)
Celgard 2500	6.95	103	57
LA-PEO-3-2	5.86	202	3.3
LA-PAM-3-2	8.36	246	3.3
LA-PEO-PAM-2-1-1	6.53	294	3.1
LA-PEO-PAM-3-1-1	9.88	375	3.0
LA-PEO-PAM-4-1-1	4.75	128	4.7

Table. S4 Experimental data of Lithium-ion transference number

Composite electrolyte	R_{io} (Ω)	R_{is} (Ω)	I_0 (μA)	I_s (μA)	ΔV (mV)	t_{Li^+}
LA-PEO-PAM-3-1-1	73.50	71.55	120.51	114.25	10	0.59
LA-PEO-3-2	364.92	360.80	24.21	22.55	10	0.58
LA-PAM-3-2	64.11	60.41	139.47	136.19	10	0.58
PEO-PAM-2-2	110.29	104.74	84.47	80.06	10	0.40
LE	42.27	37.86	205.19	197.11	10	0.42

Table. S5 Electrochemical properties at room temperature of gel polymer electrolytes reported in works of literature

GPE	σ **(S cm^{-1})**	t_{Li^+}	σ_{Li^+} **(S cm^{-1}, $\sigma \times t_{Li^+}$)**	**LFP/Li cell**	**Ref.**
3D-BGPE	8.40×10^{-4}	0.76	6.38×10^{-4}	125 mAh g^{-1} after 400 cycles at 0.5 C	1
Cellulose/PEG	3.31×10^{-3}	0.48	1.59×10^{-3}	~	2
Bacterial cellulose/LLTO	1.54×10^{-3}	0.88	1.36×10^{-3}	149 mAh g^{-1} after 100 cycles at 0.2 C	3
es-LiSPCE-s	2.52×10^{-3}	0.52	1.31×10^{-3}	110 mAh g^{-1} after 1500 cycles at 6 C	4
es-PVPSI	6.80×10^{-4}	0.85	5.78×10^{-4}	100 mAh g^{-1} after 1000 cycles at 1 C	5
PVDF-HFP/MnO_2	2.27×10^{-3}	~	~	~	6
PBA-20	4.20×10^{-4}	0.63	2.65×10^{-4}	145 mAh g^{-1} after 500 cycles at 0.5 C	7
SiO_2-(PEO-TDI-PPO)	1.32×10^{-3}	0.44	5.81×10^{-4}	148 mAh g^{-1} after 100 cycles at 0.5 C	8
PVDF-HFP/LLZTO	5.45×10^{-4}	0.58	3.16×10^{-4}	117 mAh g^{-1} after 350 cycles at 1 C	9
PMIA@PVDF-HFP/Al_2O_3-10	9.08×10^{-4}	~	~	100 mAh g^{-1} after 600 cycles at 1 C	10
PCUMA	1.27×10^{-3}	0.44	5.59×10^{-4}	~	11
PEGDE/SBMA	1.29×10^{-3}	0.63	8.13×10^{-4}	118 mAh g^{-1} after 200 cycles at 0.5 C	12
PDEIm/PVDF-HFP	1.78×10^{-3}	0.42	7.48×10^{-4}	125 mAh g^{-1} after 200 cycles at 4 C	13
Electrospinning LA-PEO-PAM-3-1-1	2.86×10^{-3}	0.59	1.69×10^{-3}	100 mAh g^{-1} after 1000 cycles at 10 C	This work

References

1. K. Dai, C. Ma, Y. Feng, L. Zhou, G. Kuang, Y. Zhang, Y. Lai, X. Cui and W. Wei, *Journal of Materials Chemistry A*, 2019, **7**, 18547-18557.
2. L. Zhao, J. Fu, Z. Du, X. Jia, Y. Qu, F. Yu, J. Du and Y. Chen, *Journal of Membrane Science*, 2020, **593**.
3. C. Ding, X. Fu, H. Li, J. Yang, J.-L. Lan, Y. Yu, W.-H. Zhong and X. Yang, *Advanced Functional Materials*, 2019, **29**, 1904547.
4. Y. He, J. Wang, Y. Zhang, S. Huo, D. Zeng, Y. Lu, Z. Liu, D. Wang and H. Cheng, *Journal of Materials Chemistry A*, 2020, **8**, 2518-2528.
5. C. Li, B. Qin, Y. Zhang, A. Varzi, S. Passerini, J. Wang, J. Dong, D. Zeng, Z. Liu and H. Cheng, *Advanced Energy Materials*, 2019, **9**.
6. H. Zhao, N. Deng, W. Kang and B. Cheng, *Chemical Engineering Journal*, 2020, **390**, 124571.
7. G. Zhou, X. Lin, J. Liu, J. Yu, J. Wu, H. M. Law, Z. Wang and F. Ciucci, *Energy Storage Materials*, 2021, **34**, 629-639.
8. S. Tang, Q. Lan, L. Xu, J. Liang, P. Lou, C. Liu, L. Mai, Y.-C. Cao and S. Cheng, *Nano Energy*, 2020, **71**, 104600.
9. Y. Xu, L. Gao, X. Wu, S. Zhang, X. Wang, C. Gu, X. Xia, X. Kong and J. Tu, *ACS Applied Materials & Interfaces*, 2021, **13**, 23743-23750.
10. L. Wang, J. Yan, R. Zhang, Y. Li, W. Shen, J. Zhang, M. Zhong and S. Guo, *ACS Applied Materials & Interfaces*, 2021, **13**, 9875-9884.
11. R. Hu, H. Qiu, H. Zhang, P. Wang, X. Du, J. Ma, T. Wu, C. Lu, X. Zhou and G. Cui, *Small*, 2020, **16**, 1907163.
12. G. Li, X. Guan, A. Wang, C. Wang and J. Luo, *Energy Storage Materials*, 2020, **24**, 574-578.
13. Z. Hu, J. Chen, Y. Guo, J. Zhu, X. Qu, W. Niu and X. Liu, *Journal of Membrane Science*, 2020, **599**, 117827.